Journal of Photonics for Energy

PhotonicsforEnergy.SPIEDigitalLibrary.org

All-optical augmentation of solar cells using a combination of up- and downconversion

Murad J. Y. Tayebjee
Akshay Rao
Timothy W. Schmidt

SPIE.

Murad J. Y. Tayebjee, Akshay Rao, Timothy W. Schmidt, "All-optical augmentation of solar cells using a combination of up- and downconversion," *J. Photon. Energy* **8**(2), 022007 (2018), doi: 10.1117/1.JPE.8.022007.

All-optical augmentation of solar cells using a combination of up- and downconversion

Murad J. Y. Tayebjee,[a,*] Akshay Rao,[a] and Timothy W. Schmidt[b]
[a]University of Cambridge, Cavendish Laboratory, Cambridge, United Kingdom
[b]UNSW Sydney, ARC Centre of Excellence in Exciton Science, School of Chemistry, New South Wales, Australia

Abstract. The limiting efficiency of a solar cell enhanced by both up- and downconversion is calculated to be 44.6% under one sun illumination using a detailed balance formalism. We show that solar cells are enhanced by both spectral conversion and photon recycling. This device architecture has the advantage of being able to enhance existing technologies after relatively few modifications. Importantly, we show that this device architecture's limiting efficiency peaks close to the band gap of silicon, unlike other spectral converters with three absorbing thresholds. © *2018 Society of Photo-Optical Instrumentation Engineers (SPIE)* [DOI: 10.1117/1.JPE.8.022007]

Keywords: spectral conversion; solar cells; limiting efficiencies; upconversion; downconversion.

Paper 18011SS received Jan. 18, 2018; accepted for publication Mar. 7, 2018; published online Mar. 28, 2018.

1 Introduction

As silicon and other conventional photovoltaic technologies become commonplace in many energy markets, there is an effort to innovate past this first generation of devices.[1,2] With the exception of hot carrier devices, high efficiency concepts exploit multiple absorbing thresholds to more effectively harvest the solar spectrum. These multiple threshold approaches can broadly be drawn into three categories: tandem solar cells,[3,4] devices where multiple thresholds are incorporated within a single absorbing layer,[5,6] spectral splitting to multiple cells,[7] and conventional cells augmented by all-optical spectral conversion devices.[8–10] The former three approaches require the development of completely new technologies whereas the latter can, in principle, be applied to existing commercially viable technologies. These all-optical approaches, using down- and/or upconversion, are attractive given the highly engineered nature of commercial solar cell technologies that have been optimized over many decades.

Downconversion, or photon fission, is the absorption of a single high-energy photon followed by the radiation of multiple low-energy photons. Upconversion, or photon fusion, is the reverse process whereby multiple low-energy photons are absorbed followed by the emission of a single high-energy photon. Both spectral conversion techniques have been approached using organic materials, quantum dots, and/or rare-earth materials.

Previous limiting efficiency calculations have been focused on augmenting a solar cell (SC) with either an upconverter (UC) or a downconverter (DC).[8–11] In this article, we present a detailed balance calculation of the limiting efficiencies of an ideal solar cell under AM1.5G illumination enhanced by both an UC and a DC (DC/SC/UC), as shown in Fig. 1(a). The work is compared with previous calculations for UC and DC systems and the current state of technology is briefly reviewed in light of the present results.

*Address all correspondence to: Murad J. Y. Tayebjee, E-mail: mjyt2@cam.ac.uk

1947-7988/2018/$25.00 © 2018 SPIE

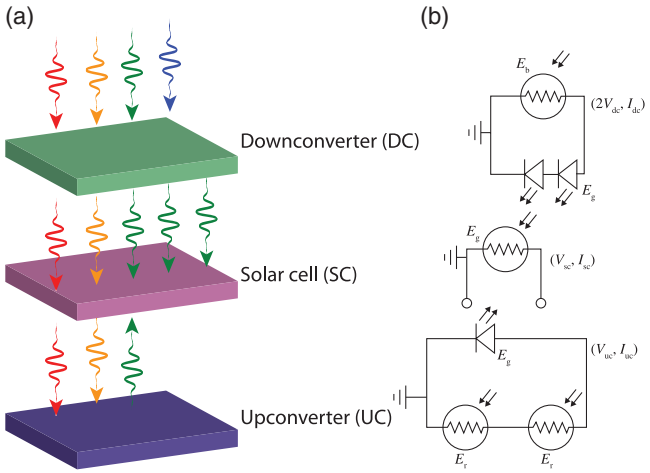

Fig. 1 (a) Architecture of a solar cell augmented by both an upconverter and a downconverter. (b) Equivalent circuit of the DC/SC/UC device.

2 Method

2.1 *Idealized Device*

We approach this problem in a similar manner to previous calculations.[8–10] In the following, there are three absorbing thresholds of interest: E_r, E_g, and E_b (denoting "red," "green," and "blue"). We model an idealized device, where the solar cell absorbs all radiation with energy greater than its band gap, E_g. The DC has two absorbing ranges, $E_g < E < E_b$ and $E > E_b$. Photons with energy in excess of E_b may be downconverted into two photons, which are emitted at E_g. Similarly, the UC has two absorbing ranges, $E_r < E < E_g$ and $E > E_g$. Two photons may be absorbed at the E_r threshold and upconverted into a single photon with energy E_g. All absorption events are assumed to have unit absorptivity and the solar cell has infinite carrier mobility.

2.2 *Detailed Balance Model*

The rates of absorption and the Einstein A coefficients governing spontaneous emission are, respectively, given by

$$k_r = \int_{E_r}^{E_g} F\mathrm{d}E; \quad k_g = \int_{E_g}^{E_b} F\mathrm{d}E; \quad k_b = \int_{E_b}^{\infty} F\mathrm{d}E, \tag{1}$$

$$k_i' = \frac{(k_B T)^3}{4\pi^2 \hbar^3 c^2}\left[\left(\frac{E_i}{k_B T}\right)^2 + 2\left(\frac{E_i}{k_B T}\right) + 2\right], \tag{2}$$

where F denotes the solar spectrum in photons/m^2/s/J and $T = 300$ K is the temperature of the cell. The speed of light, the reduced Planck constant, and Boltzmann constant are denoted in standard notation. Equation (2) is a simplification of the generalized Planck Law and is valid if $E_i \gg k_B T$.[12] The étendue of emission is given by $\epsilon = \pi n_r^2 \sin(\theta)$, where n_r is the refractive index of the medium, where light is being emitted into and θ is the half angle over which emission is occurring. In Eq. (2), $\epsilon_{\mathrm{ext}} = \pi$ has been used to simulate emission into air over a hemisphere.[8]

We use an equivalent circuit model,[8,9] where spectral converters are modeled as light-emitting diodes (LEDs) that are powered by solar cells, as shown in Fig. 1(b). The DC is modeled as a photovoltaic cell with band gap E_b, which powers two LEDs of band gap E_g and half the device area. (This is equivalent to modeling a circuit with a band gap, E_b, connected to a DC-downconverter and a single LED with band gap E_g).[13] Conversely, the UC is modeled as two cells of band gap E_r connected in series powering an LED of twice the area with bandgap E_g. The idealized device stack has the same refractive index throughout to eliminate reflections at interfaces.

The current passing through the spectral converters is

$$\begin{aligned} I_{\mathrm{dc}}/e &= I_{\mathrm{dc,cell}}/e = I_{\mathrm{dc,LED}}/e \\ &= k_b - (n_r^2+1)k_b' \frac{x_{\mathrm{dc}}^2}{x_b} \\ &= 0.5\left[-k_g - k_g' n_r^2 \frac{x_{\mathrm{sc}}}{x_g} + (n_r^2+1)k_g' \frac{x_{\mathrm{dc}}}{x_g}\right] \end{aligned} \tag{3}$$

and

$$\begin{aligned} I_{\mathrm{uc}}/e &= I_{\mathrm{uc,cell}}/e = I_{\mathrm{uc,LED}}/e \\ &= 0.5\left(k_r - k_r' \frac{x_{\mathrm{uc}}^{0.5}}{x_r}\right) \\ &= -k_g' n_r^2 \frac{x_{\mathrm{sc}}}{x_g} + n_r^2 k_g' \frac{x_{\mathrm{uc}}}{x_g}, \end{aligned} \tag{4}$$

where x_i is $\exp(\frac{E_i}{k_B T})$; $x_{\mathrm{sc,dc,uc}}$ are related to the voltages of the solar cell, downconverter, and upconverter by $\exp(\frac{V_{\mathrm{sc,dc,uc}}}{k_B T})$. The elementary charge is denoted as e. The refractive index term is required to account for the enhanced étendue of emission within the device, $\epsilon_{\mathrm{int}} = n_r^2 \pi$, where n_r was taken to be 3.6, in line with previous work.[8,9,14,15] The current passing through the solar cell is

$$\frac{I_{\mathrm{sc}}}{e} = \Phi_{\mathrm{dc}} + \Phi_{\mathrm{uc}} - 2k_g' n_r^2 \frac{x_{\mathrm{sc}}}{x_g}, \tag{5}$$

where the factor of 2 in the final term is required because the SC is bifacial. We define the photon flux passing from the spectral converters to the SC as

$$\Phi_{\mathrm{dc}} = n_r^2 k_g' \frac{x_{\mathrm{dc}}}{x_g} + n_r^2 k_b' \frac{x_{\mathrm{dc}}^2}{x_b}, \tag{6}$$

$$\Phi_{\mathrm{uc}} = n_r^2 k_g' \frac{x_{\mathrm{uc}}}{x_g}. \tag{7}$$

Finally, the efficiency of the device is taken as the maximum power, $P = I_{\mathrm{sc}} V$, divided by the total integrated solar spectrum.

3 Results

Figure 2(a) shows the maximum efficiency of the DC/SC/UC device as a function of E_g. The limiting efficiency exceeds the Shockley–Queisser limit significantly for all band gaps. The maximum efficiency of 44.6% was found at thresholds of 0.92, 1.38, and 2.61 eV. It is interesting to note that the ideal band gap of the DC is less than twice the SC band gap indicating endothermic downconversion, as has been previously observed in singlet fission materials. For comparison, previously calculated DC- and UC-augmented limiting efficiencies are also included.[14]

Unsurprisingly, the DC/SC and SC/UC devices are outperformed by the DC/SC/UC at intermediate band gaps. The DC/SC outperforms the DC/SC/UC at very low band gaps because the emission from the SC is unifacial in the former and bifacial in the latter. The SC/UC outperformed the DC/SC/UC at wide band gaps since the SC in the latter architecture is only illuminated by the DC emission rather than direct solar illumination. The maximum efficiency of the UC/SC is 43.4% at $E_g = 1.76$, which is only slightly outperformed by the DC/SC/UC. However, the range of band gaps that the DC/SC/UC is >40% is much broader than the SC/UC.

As the DC/SC/UC has three absorbing thresholds, it is also interesting to compare these results to a solar cell augmented by an asymmetric UC (SC/a-UC). This is an UC with two low-energy absorbing thresholds and a single high-energy emitting threshold, such as an

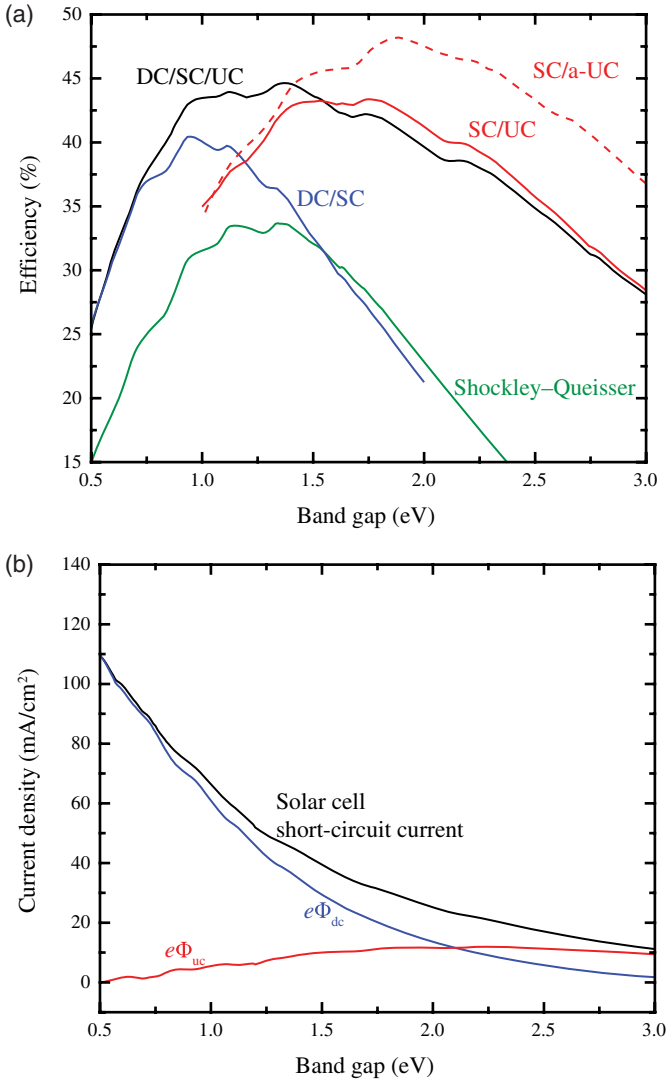

Fig. 2 (a) Limiting efficiencies for the DC/SC/UC as a function of band gap. The limiting efficiency of DC/SC, SC/UC, SC/a-UC, and the Shockley–Queisser limit are shown for comparison. (b) The short-circuit current density generated by the SC and the photon flux generated by the spectral energy converters, $e\Phi$.

intermediate band device. The SC/a-UC has a limiting efficiency of 48.2%, which significantly exceeds the DC/SC/UC. Further the SC/a-UC is highly efficient over a broad range of band gaps. However, there exist no experimental efforts that have been able to achieve this efficiently under solar illumination. Moreover, the maximum efficiency of the DC/SC/UC exceeds that of the SC/a-UC at the silicon band gap, 1.11 eV, which is important from a practical standpoint. This will be further discussed in Sec. 4.

Figure 2(b) shows the short circuit current of the idealized SC and the photon fluxes of the spectral energy converters, Φ_{dc} and Φ_{uc}, as a function of E_g. The DC(UC) produces a larger flux at smaller(larger) band gaps. Note that the flux from the DC includes both down-converted and direct photoluminescence from E_g, so nonzero fluxes are still produced at large band gaps.

The current–voltage characteristics of the individual components of the DC/SC/UC are plotted in solid lines in Fig. 3(a) with powers plotted in dashed lines. Considering Eqs. (6) and (7), we note that the spectral converters produce a greater flux at higher voltages.

The spectral converter voltage is shown in Fig. 3(b) as a function of SC operating voltage. Solving quadratic Eqs. (3) and (4) yields

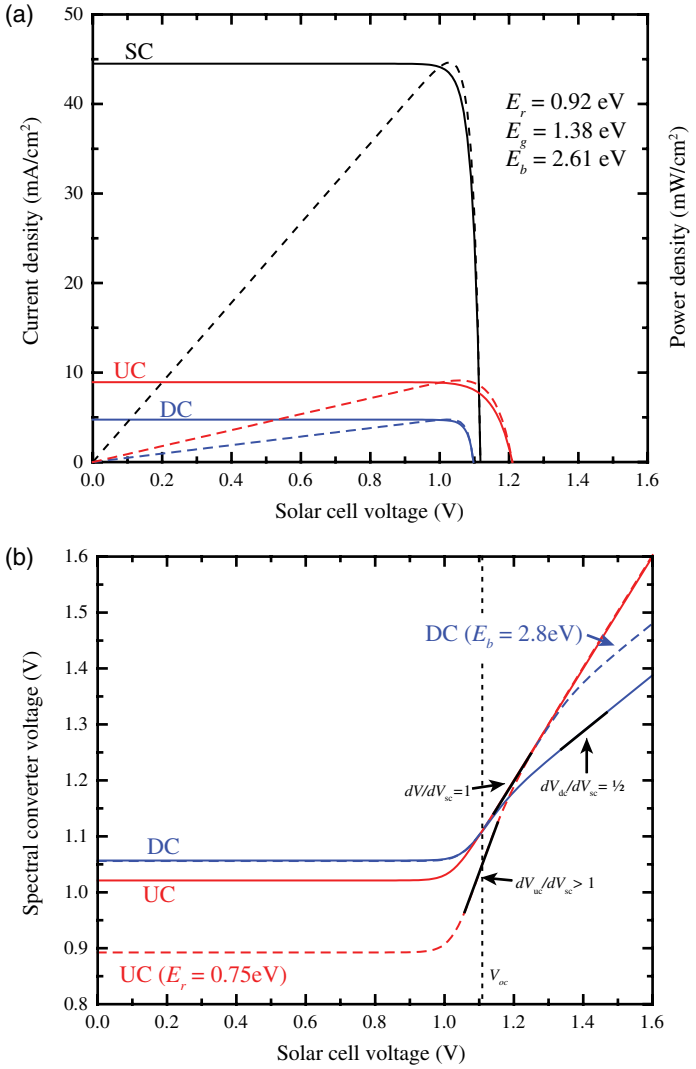

Fig. 3 (a) The currents of the components of the equivalent circuits in Eqs. (3)–(5) and Fig. 1(b) for the ideal device. Power densities are shown as dashed lines. (b) The voltages of the DC and UC as a function of the SC voltage.

$$x_{\mathrm{dc}} = \frac{x_b\left[\sqrt{(1+n_r^2)(k_g'^2 x_b + 16k_b k_b' x_g^2 + 8k_g k_b' x_g^2 + k_g'^2 n_r^2 x_b + 8k_b' k_g' n_r^2 x_g x_{\mathrm{sc}})/x_b} - k_g'(1+n_r^2)\right]}{4k_b' x_g (1+n_r^2)}, \tag{8}$$

$$x_{\mathrm{uc}} = \frac{\left(\sqrt{16x_{\mathrm{sc}}k_g'^2 n_r^2 x_r^2 + 8k_r k_g' x_g x_r^2 + k_r'^2 n_r^2 x_g^2} - k_r' n_r x_g\right)^2}{16k_g'^2 n_r^2 x_r^2}. \tag{9}$$

As the voltages of the spectral converters depend on the emission from the SC, it follows from Eqs. (8) and (9) that there are three regimes that arise from the solutions of quadratic equations of x_{dc} and $x_{\mathrm{uc}}^{0.5}$, respectively. At low values of x_{sc}, x_{dc}, and x_{uc} do not change as the constants in Eqs. (8) and (9) dominate. At intermediate values of x_{sc}, we are in a regime where $\frac{dV_{\mathrm{dc}}}{dV_{\mathrm{sc}}} = 1$ and $\frac{dV_{\mathrm{uc}}}{dV_{\mathrm{sc}}} = 2$. Finally, at higher voltages, exceeding the open-circuit voltage of the solar cell (i.e., where the solar cell is operating as an LED pumping the spectral converters) we reach the regime where $\frac{dV_{\mathrm{dc}}}{dV_{\mathrm{sc}}} = 0.5$ and $\frac{dV_{\mathrm{uc}}}{dV_{\mathrm{sc}}} = 1$ as the DC and UC voltages become governed by the terms $\frac{x_{\mathrm{dc}}^2}{x_b}$ and

$\frac{x_{uc}}{x_g}$ in Eqs. (3) and (4). To further elucidate these changes in gradient, we also include the voltages of non-ideal devices as dashed lines in Fig. 3(b). Here, E_r is decreased to 0.75 eV, the extent of the $\frac{dV_{uc}}{dV_{sc}} = 2$ regime is enhanced since x_{sc} is diminished versus the other terms in the discriminant. Similarly, when E_b is increased to 2.8 eV the $\frac{dV_{dc}}{dV_{sc}} = 1$ regime exists over a larger extent of Fig. 3(b).

4 Discussion

The limiting efficiencies calculated in this work are lower than electrically contacted multiple threshold approaches. This is due to the extra radiative step which effectively limits the rate of conversion of solar photons into electrical current. However, the attraction of all-optical approaches lies in the fact that contact engineering is not required and, with the exception of parallel tandems,[16] spectral converters are far less sensitive to changes in the solar spectrum.

The ultimate goal of fabricating spectral converters is to enhance current photovoltaic technologies. In Fig. 4, we establish the dependence of the current density and maximum power for an idealized solar cell with the same band gap as silicon ($E_g = 1.11$ eV) as a function of energy thresholds E_r and E_b. Figure 4(a) shows the flux of the spectral converters when the SC is operating under short-circuit conditions. Unsurprisingly, the flux of the DC and UC only varies with E_b and E_r, respectively, and the current in the solar cell under short-circuit conditions is

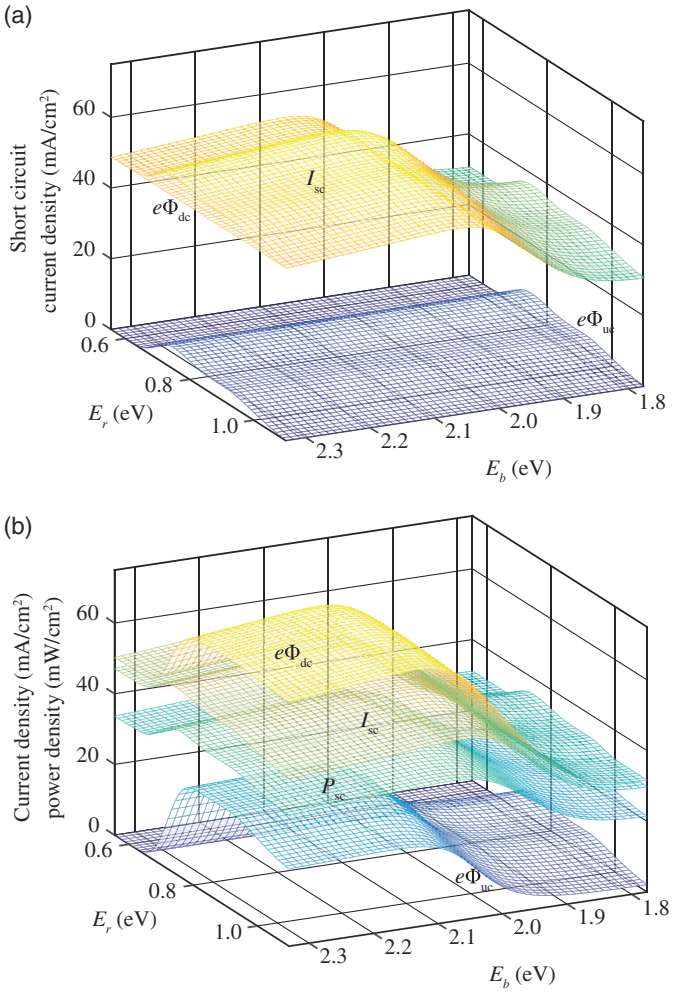

Fig. 4 Current density, power density, and photon flux from spectral converters for a solar cell with $E_g = 1.11$ eV operating under (a) short circuit and (b) maximum power conditions. The photon fluxes from the spectral converters, $e\Phi$, are given in units of mA/cm^2.

$\frac{I_{sc}}{e} = \Phi_{dc} + \Phi_{uc}$. Although the contribution of the UC is small compared with that of the DC, it is clear from Fig. 2(a) that the overall enhancement of the device is significant.

Figure 4(b) shows the same data but for a device operating at its maximum power point. Here, the contribution from the UC is more significant. This can be understood by considering Eqs. (3)–(7). As the SC voltage is increased, the chemical potential in the spectral converters is also increased [see Fig. 3(b)] and this results in a greater flux from the spectral converters [see Eqs. (6) and (7)]. Further, the variation of the voltage of the solar cell as a function of both E_r and E_b results in a variation in the flux generated by both of the spectral converters with both E_r and E_b. In other words, the chemical potential of the UC and DC is inextricably linked.

There is a large plateau of high currents (>42 mA/cm^2) in the approximate region $0.7 < E_r < 0.95$ eV and $2.0 < E_b < 2.2$ eV. In this regime, Φ_{uc} arises from exothermic photon fusion and re-emitted photons that are absorbed from the solar cell; and Φ_{dc} arises from endothermic photon fission and also from recycling photons emitted from the solar cell. Photon recycling is effective since the DC and UC absorb light emitted from the SC. We have simulated a refractive index matched DC/SC/UC stack with $n_r = 3.6$. This results in $n_r^2/(1+n_r^2) \sim 93\%$ of emission from the DC being directed back into the device.

From a technological standpoint, the UC requires a low-energy absorber that can undergo fusion and the DC requires a high-energy absorber that can undergo fission. Both spectral converters required an emitter at E_g, which opens the possibility of using the same emitter in both the UC and the DC.

Presently, the only available materials capable of upconverting from below the bandgap of crystalline silicon are the rare-Earth doped inorganic compounds. Owing to the similarity in ion-size and chemistry within the lanthanoids, erbium is easily doped into the structure of optically benign yttrium salts, and a ~20% to 30% doping level has emerged as optimal.[17] The accepted figure of merit for an upconverting solar cell is the enhancement of short-circuit current density due to upconversion, corrected for any solar concentration, ΔJ_{UC}.[18,19] The highest ΔJ_{UC} so far reported for crystalline silicon cells is 8.9×10^{-3} mA/cm^2,[20] representing a 0.55% relative increase in solar cell efficiency.

At present, a downconversion system with efficiency above 100% has not been demonstrated. Singlet fission materials such as tetracene (and tetracene derivatives) have the right energetics for such a device, absorbing photons above 2.2 eV and producing two triplets at 1.3 eV. These triplets can then be efficiently transferred into inorganic quantum dots such as PbS,[21,22] where the exciton can undergo radiative recombination and emit low-energy photons. The challenge is to maintain high photoluminescence quantum efficiency in the inorganic quantum dot while allowing for efficient harvesting of the triplets. Full details of the materials requirements and challenges can be found in a recent review.[23]

It should be noted that, while an all-optical approach avoids the need for further electrical contacts, the refractive index of the components of the device should be matched. If the refracting indices of the SC, DC, and UC do not match, we expect reflections at these interfaces, which will generate losses in the device. Practically speaking, this may be overcome by adding antireflective coatings. Moreover, a departure from the refractive index value used here (3.6) will alter the results; a downconverter directs $\frac{n_r^2}{n_r^2+1}$ of its radiation toward the solar cell. If n_r is decreased, radiative losses out of the front of the DC will increase.

5 Conclusions

The economics of single threshold solar cell technology has improved over the last few decades to the point where it is now competitive with fossil fuel electricity generation. The incorporation of spectral converters could be used to achieve a step-advance in the cost per watt of these devices. We have shown here that, when used in tandem, up- and down-converters significantly enhance the efficiency of solar cells. Considering silicon, the current market leader, the DC/SC/UC raises the efficiency limit from 33% for an unaugmented device to 44% with band gaps $E_r = 0.76$ and $E_b = 2.08$ eV. Interestingly, this increase is not only due to photon fission or fusion, but also because spectral converters recycle photons that are emitted by solar cells.

Acknowledgments

We acknowledge EPSRC and the Winton Programme for the Physics of Sustainability for funding. This work was supported by a Marie Sklodowska Curie Individual Fellowship (705113). T.W.S. acknowledges the Australian Research Council for a Future Fellowship (FT130100177). This work was supported by the Australian Research Council (Centre of Excellence in Exciton Science CE170100026).

References

1. M. A. Green, *Third Generation Photovoltaics: Advanced Solar Energy Conversion*, Springer-Verlag, Berlin, Germany (2003).
2. M. A. Green, "Third generation photovoltaics: solar cells for 2020 and beyond," *Phys. E* **14**, 65–70 (2002).
3. A. De Vos, "Detailed balance limit of the efficiency of tandem solar cells," *J. Phys. D-Appl. Phys.* **13**, 839–846 (1980).
4. S. P. Bremner, M. Y. Levy, and C. B. Honsberg, "Analysis of tandem solar cell efficiencies under AM1.5G spectrum using a rapid flux calculation method," *Prog. Photovoltaics Res. Appl.* **16**, 225–233 (2008).
5. A. Luque and A. Martí, "Increasing the efficiency of ideal solar cells by photon induced transitions at intermediate levels," *Phys. Rev. Lett.* **78**, 5014–5017 (1997).
6. S. P. Bremner, M. Y. Levy, and C. B. Honsberg, "Limiting efficiency of an intermediate band solar cell under a terrestrial spectrum," *Appl. Phys. Lett.* **92**, 171110 (2008).
7. A. G. Imenes and D. R. Mills, "Spectral beam splitting technology for increased conversion efficiency in solar concentrating systems: a review," *Sol. Energy Mater. Sol. Cells* **84**, 19–69 (2006).
8. T. Trupke, M. A. Green, and P. Wurfel, "Improving solar cell efficiencies by down-conversion of high-energy photons," *J. Appl. Phys.* **92**, 1668–1674 (2002).
9. T. Trupke, M. A. Green, and P. Wurfel, "Improving solar cell efficiencies by up-conversion of sub-band-gap light," *J. Appl. Phys.* **92**, 4117–4122 (2002).
10. T. Trupke et al., "Efficiency enhancement of solar cells by luminescent up-conversion of sunlight," *Sol. Energy Mater. Sol. Cells* **90**, 3327–3338 (2006).
11. T. Markvart and P. T. Landsberg, "Thermodynamics and reciprocity of solar energy conversion," *Phys. E* **14**, 71–77 (2002).
12. L. C. Hirst and N. J. Ekins-Daukes, "Fundamental losses in solar cells," *Prog. Photovoltaics Res. Appl.* **19**, 286–293 (2010).
13. M. J. Y. Tayebjee, A. A. Gray-Weale, and T. W. Schmidt, "Thermodynamic limit of exciton fission solar cell efficiency," *J. Phys. Chem. Lett.* **3**, 2749–2754 (2012).
14. M. J. Y. Tayebjee, D. R. McCamey, and T. W. Schmidt, "Beyond Shockley–Queisser: molecular approaches to high-efficiency photovoltaics," *J. Phys. Chem. Lett.* **6**, 2367–2378 (2015).
15. M. J. Y. Tayebjee, T. W. Schmidt, and G. Conibeer, "Downconversion," in *Comprehensive Renewable Energy*, A. Sayigh, Ed., pp. 549–561, Elsevier (2012).
16. L. M. Pazos-Outón et al., "A silicon-singlet fission tandem solar cell exceeding 100% external quantum efficiency with high spectral stability," *ACS Energy Lett.* **2**, 476–480 (2017).
17. J. C. Goldschmidt and S. Fischer, "Upconversion for photovoltaics—a review of materials, devices and concepts for performance enhancement," *Adv. Opt. Mater.* **3**, 510–535 (2015).
18. T. F. Schulze and T. W. Schmidt, "Photochemical upconversion: present status and prospects for its application to solar energy conversion," *Energy Environ. Sci.* **8**, 103–125 (2015).
19. L. Frazer, J. K. Gallaher, and T. W. Schmidt, "Optimizing the efficiency of solar photon upconversion," *ACS Energy Lett.* **2**, 1346–1354 (2017).
20. S. Fischer et al., "Record efficient upconverter solar cell devices with optimized bifacial silicon solar cells and monocrystalline BaY_2F_8:30% Er^{3+} upconverter," *Sol. Energy Mater. Sol. Cells* **136**, 127–134 (2015).

21. N. J. Thompson et al., "Energy harvesting of non-emissive triplet excitons in tetracene by emissive PbS nanocrystals," *Nat. Mater.* **13**, 1039–1043 (2014).
22. M. Tabachnyk et al., "Resonant energy transfer of triplet excitons from pentacene to PbSe nanocrystals," *Nat. Mater.* **13**, 1033–1038 (2014).
23. A. Rao and R. H. Friend, "Harnessing singlet exciton fission to break the Shockley–Queisser limit," *Nat. Rev. Mater.* **2**, 17063 (2017).

Murad J. Y. Tayebjee is a Marie Sklodowska Curie Fellow at the Cavendish Laboratory, University of Cambridge. He will shortly take up a Senior Lectureship at the School of Photovoltaic and Renewable Energy Engineering at The University of New South Wales. His research focus is the optical spectroscopy of artificial light harvesting systems.

Akshay Rao is leads a research group at the Cavendish Laboratory, University of Cambridge where he is an EPSRC Early Career Fellow and Winton Advanced Research Fellow. His research interests include the electronic and optical properties of molecular semiconductors, quantum dots and 2D semiconductors. He has worked extensively on organic and nanostructured inorganic semiconductors, using ultrafast spectroscopy to elucidate the how charge delocalisation, ballistic motion and vibronic coupling underlie the physics of these systems.

Timothy W. Schmidt is a professor of chemistry at the University of New South Wales, in Sydney, Australia. Previous appointments include The University of Sydney, CSIRO Australia and University of Basel. His research group studies molecular spectroscopy, both in the condensed and gas phase, with applications ranging from astrophysics to renewable energy.